

Supporting information

Superhydrophilic and underwater superoleophobic zirconium-based metal-organic framework composite stainless steel mesh for oil-water separation

Yuxin Zhang, Yuanfeng Fu, *Zhenzhong Fan, Qilei Tong, Fuzhen Liu, Shanshan Liu and Yifan Zhao

The Key Laboratory of Enhanced Oil and Gas Recovery, Ministry of Education, Northeast Petroleum University, Daqing, 163318, China

Corresponding author. Email: fanzhenzhong@nepu.edu.cn

1. Comparison of different membranes

A comparative analysis was conducted between the SPU-66 composite membrane and six previously reported hydrophilic/oleophobic composite membranes in terms of oil–water separation efficiency, water flux, separation mechanism, underwater oil contact angle, and resistance to acidic and alkaline environments (Table S1). This comprehensive comparison highlights the enhanced overall performance of the SPU-66 membrane, especially under complex separation conditions, and demonstrates its strong potential for practical applications in oil–water separation technologies.

Table S1 Comparison of hydrophilic/oleophobic membranes.

Membrane	Separation efficiency (%)	Water flux (L·m ⁻² ·h ⁻¹)	Operation pressure	contact angle (°)	Acid / Alkali	quote
CMC/Uio-66-NH ₂	99.2	7430±98	strain	160	Good	5
MOF-303@SSM	99.35	1.68×10 ⁴	gravity	155	Excellent	18
GO coated mesh	98.0	3.02×10 ⁵	gravity	152	Moderate	33
Cu(OH) ₂ @ZIF-8	97.2	9×10 ⁴	gravity	155	Excellent	34
SiO ₂ nanofiber membranes	99.1	4420	gravity	136.5	Good	35
Sr-MOF	99.5	1400	gravity	134	Excellent	36
SPU-66	98.5	6.51×10 ⁵	gravity	156	Excellent	Work

References:

- 5 Ma L., Wan Y., Wang T., Liu Y., Yin Y. and Zhang L., *Langmuir*, 2022, **38**, 12499–12509.
- 18X. Yin, Y. He, T. He, H. Li, J. Wu, L. Zhou, S. Li and C. Li, *Colloids and Surfaces A: Physicochemical and Engineering Aspects*, 2023, **657**, 130515.
- 33X. Zuo, K. Chang, J. Zhao, Z. Xie, H. Tang, B. Li and Z. Chang, *J. Mater. Chem. A*, 2016, **4**, 51–58.
- 34Q. Li, W. Deng, C. Li, Q. Sun, F. Huang, Y. Zhao and S. Li, *ACS Appl. Mater. Interfaces*, 2018, **10**, 40265–40273.
- 35H. Meng, X. Pan, X. Li, H. Meng and S. Li, *ChemistrySelect*, 2023, **8**, e202300694.
- 36A. Raj, R. M. Rego, K. V. Ajeya, H.-Y. Jung, T. Altalhi, G. M. Neelgund, M. Kigga and M. D. Kurkuri, *Chemical Engineering Journal*, 2023, **453**, 139757.

2. SPU-66 synthesized section

Figure S1 corresponds to Section “2.2 Preparation” in the manuscript. It primarily illustrates the process of dopamine modification on the stainless steel mesh and the subsequent in situ growth of UiO-66 crystal on the modified mesh.

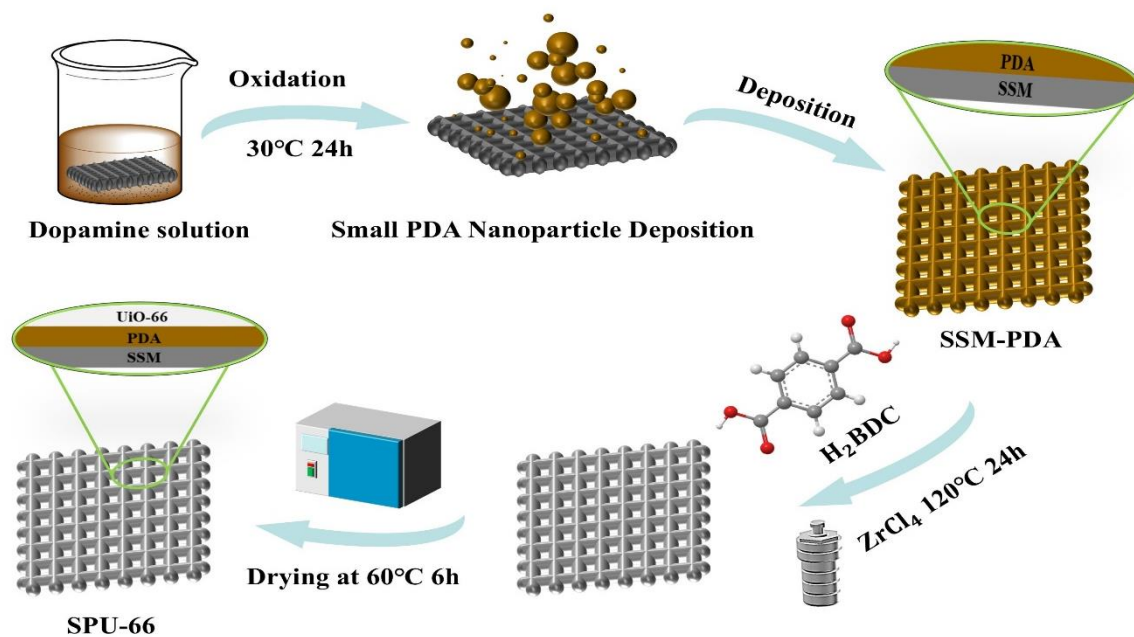


Figure S1 Preparation of SPU-66 membrane by in situ growth method.

3. Characterization section

Figures S2 and S3 correspond to Section “3.1.3 X-ray photoelectron spectroscopy” in the manuscript, and they show the spectra of Fe and Zr.

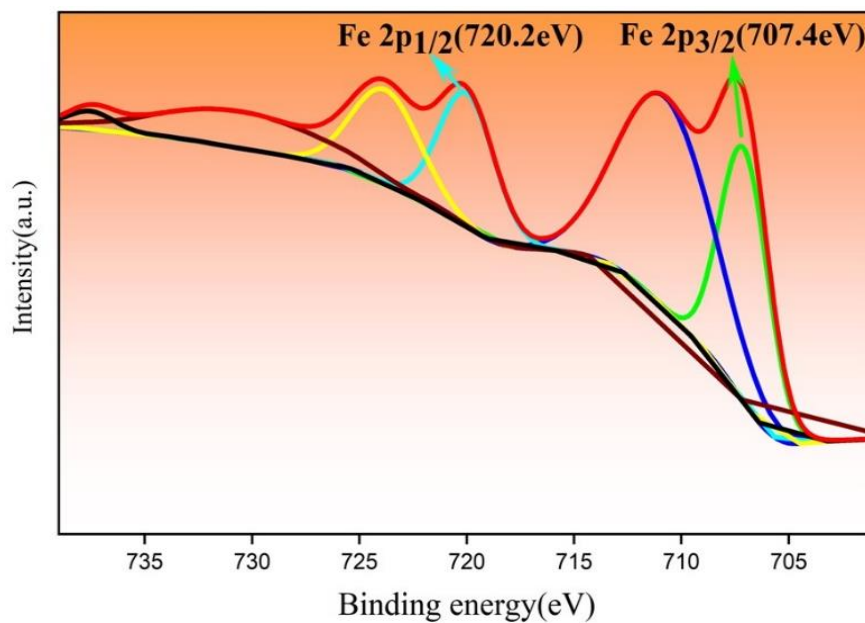


Figure S2 XPS spectra of Fe 2p for SPU-66.

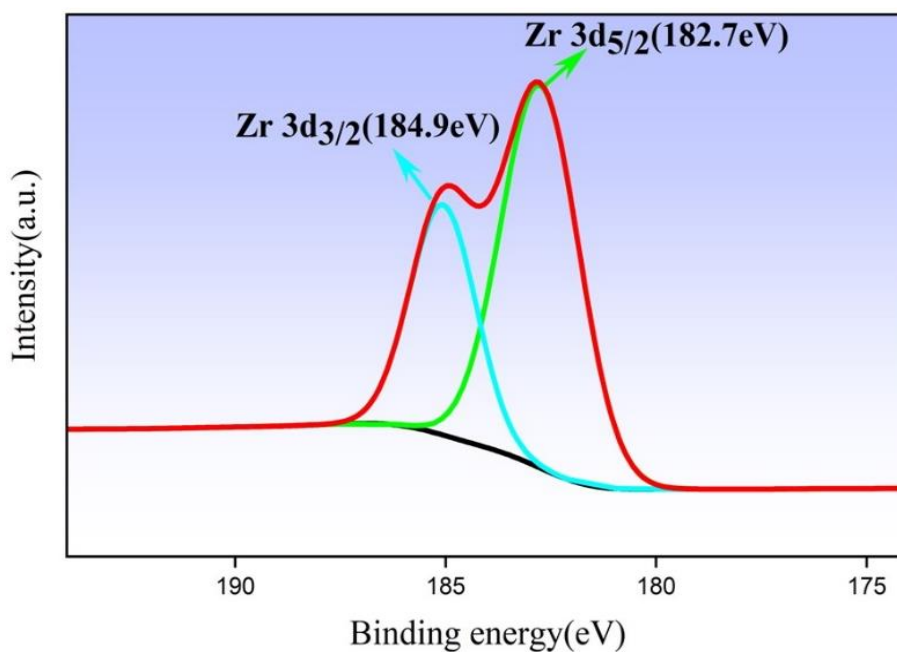


Figure S3 XPS spectra of Zr 3d for SPU-66.

Figures S4 and S5 correspond to Section “3.1.4 Energy Dispersive X-ray Spectroscopy” in the manuscript. Figure S5 shows the elemental composition of SPU-66.

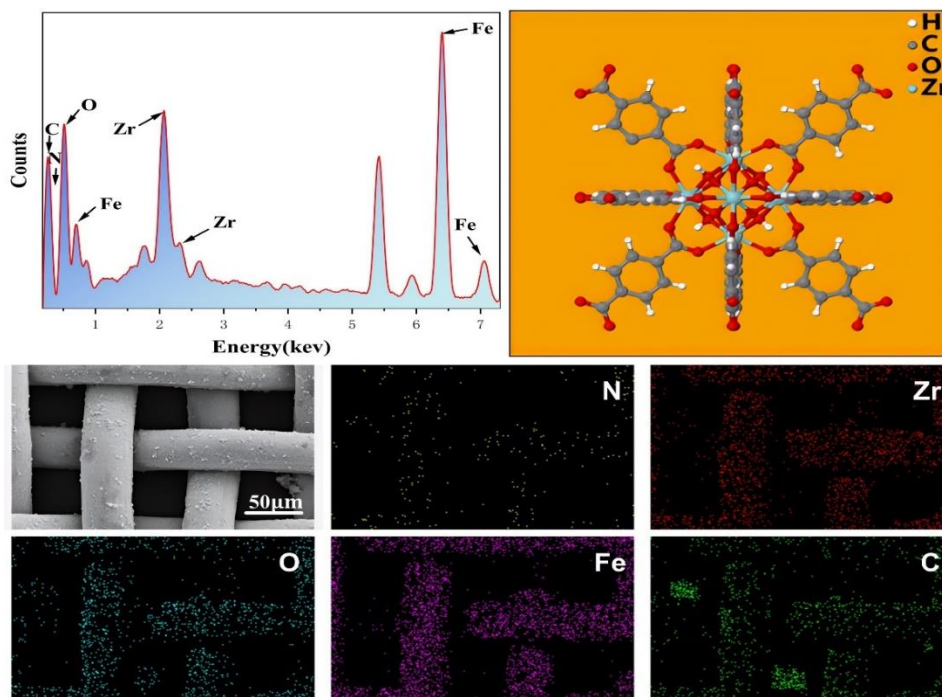


Figure S4 EDS energy spectrum and molecular structure of SPU-66.

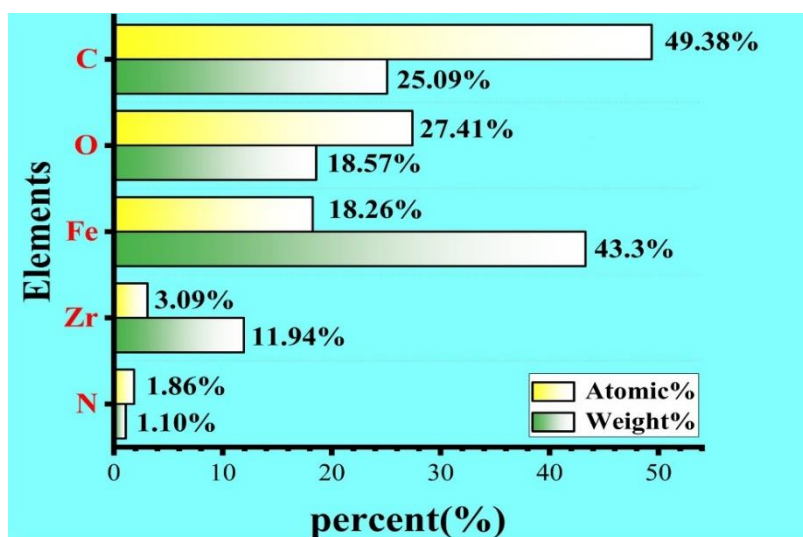


Figure S5 Percentage of the five elements.

4. Experimental section

Figures S6, S7, and S8 correspond to Section “3.3 Wettability and Separation Mechanism of SPU-66” in the manuscript. Based on the three models shown in Figure S6, the separation mechanism of the SPU-66 membrane can be analyzed. Figures S7 and S8 present the oil adhesion tests of the SPU-66 composite membrane.

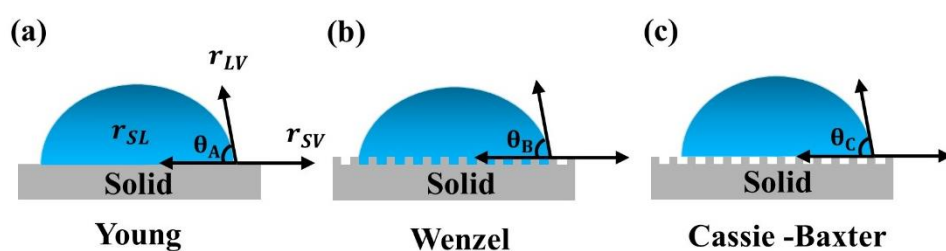


Figure S6 Wetting states of droplets in (a) Young model, (b) Wenzel model and (c) Cassie-Baxter model.



Figure S7 SPU-66 Rolling angle test.

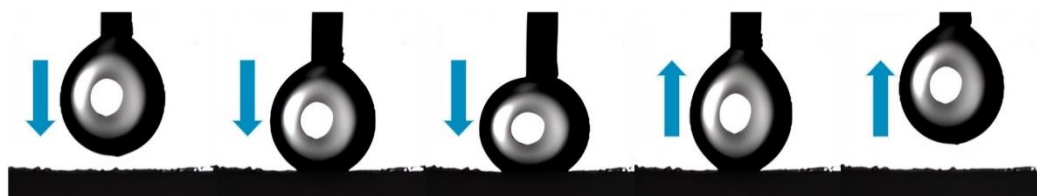


Figure S8 SPU-66 oil droplet adhesion test.